RESEARCH PAPER

Rilpivirine-loaded solid lipid nanoparticles: preparation, characterization, and *in vivo* evaluation for enhancing oral bioavailability

Mangesh Bhalekar[1], Ashwini Madgulkar[1], Aditi Pande[1], Chetashri Patil[1], Maryam Mulla[1*]

[1]Department of Pharmaceutics, AISSMS College of Pharmacy, Pune, India

ABSTRACT

Objective(s): This study aimed to improve the oral bioavailability of Rilpivirine by creating and testing Rilpivirine solid lipid nanoparticles (SLNs) to determine the impact of drug delivery on pharmacokinetics following oral treatment in Wistar rats.

Materials and Methods: Solid lipid nanoparticles (SLNs) were fabricated using a high-pressure homogenization technique, after which they were evaluated for their physicochemical properties including particle size, morphology, zeta potential, encapsulation efficiency as well as their in vitro release behaviour, ex vivo permeability, and in vivo pharmacokinetics in Wistar rats. To further understand how SLNs are taken up through the lymphatic system, an ex vivo study was carried out using an everted rat intestinal sac model.

Results: The resulting SLNs were spherical, showing an average particle size of 74.45 ± 0.84 nm with a PDI of 0.27, zeta potential -17.49 ± 0.82 mV, and an entrapment efficiency of 62.9 ± 1.2%. The SLN formulation demonstrated 84% drug release over a 24-hour period. In an ex vivo study using everted rat intestine, the SLN's apparent permeability was 34.2×10^{-6} at 37 ± 0.5 °C without chlorpromazine. This value decreased to 14.6×10^{-6} when chlorpromazine was present. Pharmacokinetic studies in rats showed the SLN formulation's AUC was 1.04 times higher than that of the pure drug suspension. Conversely, adding the lymphatic uptake inhibitor chlorpromazine reduced the SLN's AUC by 0.52-fold. The in vivo pharmacokinetic data was assessed by Dunnett's test, which indicated a significant difference ($p < 0.05$) between the RLV SLNs and the plain RLV drug.

Conclusion: Employing SLNs as a delivery vehicle appears to be a viable method for boosting the therapeutic efficacy of rilpivirine. A key reason is that SLN lymphatic uptake is important for avoiding hepatic first-pass metabolism.

Keywords: *Rilpivirine; Bioavailability; Lymphatic uptake; Solid lipid nanoparticles; Permeability; Solubility*

How to cite this article

Bhalekar M, Madgulkar A, Pande A, Patil Ch, Mulla M. Rilpivirine-loaded solid lipid nanoparticles: preparation, characterization, and in vivo evaluation for enhancing oral bioavailability. Nanomed J. 2026; 13: 1-. DOI: 10.22038/NMJ.2026.86737.2190

Corrected Proof

INTRODUCTION

HIV is a significant public health issue that has caused the deaths of 40.1 million individuals (with a range of 33.6-48.6 million). HIV remains incurable but has been manageable to certain levels owing to access to advanced diagnostic and treatment HAART, including the administration of at least three combination antiretroviral medicines, and is the standard treatment for HIV/AIDS patients [1,2]

For HIV replication, reverse transcriptase enzyme is responsible for the transcription of ssRNA into dsDNA. Rilpivirine (RPV), a second-generation non-nucleoside reverse transcriptase inhibitor (NNRTI) that inhibits HIV reverse transcriptase enzyme by binding to the enzyme and subsequently prevents viral RNA transcription [3]. It is a BCS Class II drug with high lipophilicity (log P = 4.86) and poor solubility in aqueous medium [4,5]. Its low bioavailability (32% in rats) is due to the drug's poor solubility and low dissolution rate in aqueous medium, coupled with first-pass metabolism. Different strategies, such as the formulation of nanoparticles, nanosponges, and solid dispersions, have been used to address these shortcomings [6]. SLNs (Solid lipid nanoparticles) are typically constructed with a solid lipid carrier, stabilized by surfactants, and have a particle size in the 10 to 1000 nm range. SLNs have the potential for site-specific drug administration, controlled release, enhanced bioavailability, decreased adverse effects, dosage form stability, and decreased fed/fasted variability, making them a rapidly developing nanotechnology platform. Lipid-based delivery systems improve the oral absorption of low solubility drugs, such as darunavir and efavirenz, by facilitating

* *Corresponding author:* Maryam Mulla, Department of Pharmaceutics, AISSMS College of Pharmacy, Pune411001, India. Phone: +917972906415, Email: maryammulla89@gmail.com.

Note. This manuscript was submitted on March 17, 2025; approved on November 17, 2025.

© 2026. This work is openly licensed via CC BY 4.0. This is an Open Access article distributed under the terms of the Creative Commons Attribution License (https://creativecommons.org/licenses), which permits unrestricted use, distribution, and reproduction in any medium, provided the original work is properly cited.

their entry into the lymphatic transport pathway. These systems promote the association of the drugs with chylomicrons, which are subsequently taken up by M cells in the Peyer's patches, thereby improving systemic absorption.[7–9]. Following administration, the lipid-based, nano-sized SLNs are readily taken up by lymphatic cells. This process allows a higher drug concentration to reach the lymphatic circulation, bypass first-pass metabolism, and consequently improve oral bioavailability [10].

The present investigation focused on formulating SLNs to enhance the oral absorption of rilpivirine and to elucidate lymphatic transport and improved dissolution as the key mechanisms involved.

Materials and Methods

Materials

Rilpivirine was generously supplied by Mylan Laboratories Ltd., Hyderabad, India. Glyceryl caprylate was obtained as a gift sample from Subhash Chemicals, Bhosari, Pune, while all other reagents were procured from S.D. Fine Chemicals, Mumbai, India.

Methods

Selection of lipid

Lipid selection was based on the drug's solubility within the lipid. The lipids evaluated were glyceryl monostearate, Gelucire 50/13, Compritol ATO 888, stearic acid, Precirol ATO 5, and Glyceryl Caprylate. We added 10 mg of Rilpivirine to 10 mg of the melted lipid (held at its specific melting point) under constant stirring. The test tube was kept warm in a water bath set above the lipid's melting temperature. Further, lipid was incrementally added by 10 mg with stirring and heating until a clear transparent melt was created. Lipids were added to obtain a transparent solution, and the total quantity of lipids required was noted. The lipid exhibiting the highest drug-loading capacity was selected for subsequent investigations.

Selection of the surfactant system

The selection of a surfactant is a critical component of the SLNs. Span 80, SLS, Poloxamer 188, and Tween 80 were chosen for this study. The surfactants were selected according to the mean particle size and polydispersity index (PDI) of the SLN formulations. A combination of lipids and water-soluble surfactants was used to prepare the SLN dispersions, as given in Table 1.

Preparation of Rilpivirine SLNs dispersion

We fabricated the SLNs utilizing a high-pressure homogenization (HPH) method [11). First, Rilpivirine was added to precisely weighed Glyceryl Monostearate, and this mixture was melted at a temperature 10 °C above the lipid's melting point. Glyceryl Caprylate was used as a co-solubilizer. SPAN 80, the lipid-phase surfactant, was incorporated into the lipid mixture. Tween 80 (2%) was incorporated into distilled water maintained at 70 °C to prepare the aqueous phase. The aqueous phase was combined with the lipid phase, which had been heated to an equivalent temperature, and the mixture was continuously stirred using a mechanical stirrer (Remi, India) at 1200 rpm for 15 minutes. The resulting pre-emulsion was then processed through a high-pressure homogenizer (Panda Plus, GEA, Italy) under a constant homogenization pressure of 800 bar.

Optimization of SLNs using experimental design

We optimized the SLN formulation with Design Expert Software (Version 13, State Ease. Inc, Minneapolis, USA). Table 2 represents the experimental design. The Box-Behnken design involves three factors with three levels, as shown in Table 3. To evaluate the effects of three independent variables lipid concentration, surfactant concentration, and the number of homogenization cycles each assessed at three levels, on the responses of particle size and entrapment efficiency, as well as to assess the interactions among these factors [12].

Corrected Proof

Table 1. Particle size and PDI of SLNs prepared by using various surfactant combinations

Batch	Lipid Phase Surfactant (2%)	Aqueous surfactant (2%)	Particle size(nm)	PDI
S1	SPAN 80	SLS	230	0.935
S2	SPAN 80	Poloxamer 188	203	0.761
S3	SPAN 80	Tween 80	106	0.153

Table 2. Design Layout of Box Behnken design for optimization of Rilpivirine SLNs

Sr. No	Factors			Responses
1	The concentration of lipid (gm)	-1(5g)	0(6.5g)	+1(7g)	Particle size(nm) Entrapment Efficiency (%)
2	The concentration of surfactant (%)	-1(2%)	0(2.5%)	+1(3%)	
3	No Homogenization cycles (cycles)	-1(1)	0(3)	+1(5)	

Table 3. Experimental run and responses for optimization of Rilpivirine SLNs formula using Box Behnken design

Batch No	Factor 1 A: lipid ratio	Factor 2 B: Surfactant concentration	Factor 3 C: No. of homogenization	Response 1 Particle Size	Response 2 Entrapment Efficiency
	%	%	cycles	nm	%
F1	20	3	3	47.2	57.6778
F2	20	2.5	1	129	53.9186
F3	30	2	3	235.3	65.1962
F4	30	3	3	76.64	71.4615
F5	20	2	3	99.22	56.4248
F6	30	2.5	1	157	69.8952
F7	25	3	5	38.68	58.6176
F8	20	2.5	5	50.49	56.738
F9	25	3	1	75.76	63.6299
F10	25	2.5	3	130.6	60.8105
F11	25	2	1	348.6	59.8707
F12	25	2	5	91.33	62.3768
F13	30	2.5	5	141.6	67.0758

Particle size and polydispersity index determination

We measured the SLN particle size using a Malvern Zetasizer ZS 90 (Malvern Instruments, Worcestershire, UK). Samples were diluted with distilled water before measurement. We recorded both the mean particle size and the polydispersibility index [13].

Determination of entrapment efficiency

To calculate the entrapment efficiency, 5 ml of the RPV SLN formulation was placed in an Eppendorf tube. This was centrifuged for 10 minutes at 20000 rpm. The resulting SLN pellet was separated from the clear supernatant. We then analyzed the supernatant using a spectrophotometer at 308 nm [14]. The following formula used to calculate Entrapment efficiency,

$$EE(\% = \frac{Wtotal - Wfree}{Wtotal} \times 100 \quad (1)$$

Where,

W_{total} = amount of the drug added into the formulation

W_{free} = amount of drug present in supernatant.

Preparation of RPV coarse suspension (RPV-CS)

RPV (10 mg) was suspended in a 0.5% methylcellulose solution. This was used as a control formulation in further studies.

Surface morphology by Scanning Electron Microscopy (SEM)

Surface morphology was evaluated using scanning electron microscopy. The optimized formulation was dried and examined using an SEM instrument (Nova NanoSEM NPEp303).

Differential Scanning Calorimetry (DSC)

Differential scanning calorimetry (DSC) of RPV and RPV-loaded SLNs was conducted using a HITACHI DSC 7020 instrument. The SLN samples were sealed in aluminum pans and heated at a rate of 10 °C/min under a nitrogen flow of 60 mL/min. The heating range was kept between 30-300 ˚C [14].

In-Vitro drug release study

In vitro drug release was evaluated using the dialysis bag technique. One dialysis membrane (molecular weight cut off 10000–12000 Da) was filled with SLNs dispersion and the other with a plain drug suspension [15]. A USP Apparatus II was employed using 900 mL of 0.1 N HCl containing 0.5% Tween 20 as the dissolution medium. The dissolution study was conducted at 37 ± 0.5 °C with a paddle rotation speed of 75 rpm using a standard dissolution apparatus (LabIndia, India). Samples were collected and filtered at different time intervals (0.5, 1, 2, 3, 4, 5, 6, and 12 h). The collected samples were analyzed at 280 nm using a UV–visible spectrophotometer (Shimadzu UV1780). Several kinetic models were applied to elucidate the underlying drug-release mechanism.

Ex vivo lymphatic uptake study using everted rat sac model

To examine permeability and gain a better understanding of how Rilpivirine SLNs are absorbed, an everted rat sac model was used to study its effects on the rat intestine [16]. The intestines were isolated and everted using a glass rod, after which they were mounted on an everted gut sac apparatus. To investigate the contribution of lymphatic transport, an ex vivo permeability study of the RPV-SLN formulation was conducted in the presence and absence of chlorpromazine (CPZ, 10 µg/mL), a known inhibitor of lymphatic uptake [17]. The concentration of CPZ used as a clathrin inhibitor is effective and non-toxic in this model [18,19]. Samples withdrawn from the receiver

Corrected Proof

compartment were analyzed for drug content at 280 nm using UV–visible spectrophotometry.

Papp values were calculated using the given Equation.

$$Papp = \frac{dQ/dt}{A \times Co} \qquad (2)$$

Where,

dQ/dt is the change in concentration in the intestinal sac (receiver compartment),

Co is the initial concentration of RPV present outside everted gut sac (donor compartment) and,

A is the total area of the intestinal tissue.

In-vivo pharmacokinetic studies

A pharmacokinetic study was carried out to assess the plasma absorption of rilpivirine following oral administration of the SLN dispersion. The study was conducted in fasted male Wistar rats, and the experimental protocol received approval from the Institutional Animal Ethics Committee (Approval No. CPCSEA/IAEC/PT-09/01-2K23). The animals were separated into three groups. Prior to the study, these animals were required to fast for a minimum of 12-14 hours while still having access to water.

Table 4. Animal group In-vivo pharmacokinetic study of Solid lipid Nanoparticles

Group	Dose of Drug	Number of samples (n)	Formulation
A (Control)	1 mg/kg	6	Rilpivirine suspension
B	1 mg/kg	6	Rilpivirine SLN formulation
C	1 mg/kg	6	Rilpivirine SLN formulation with lymphatic uptake blocker i.e. Chlorpromazine

All formulations were administered orally using an 18-gauge feeding needle. Blood samples were collected via the retro-orbital plexus into EDTA-coated tubes at predetermined time points (0.5, 1, 2, 4, 8, 12, 16, and 24 h). The samples were centrifuged at 3000 rpm for 20 minutes to separate plasma, which was subsequently stored at −20 °C until analysis.

Estimation of concentration of RPV in rat plasma

RPV plasma concentrations were quantified using high-performance liquid chromatography (HPLC) equipped with an Agilent PU 2080 Plus pump (India). Each plasma sample (100 µL) was placed in a centrifuge tube, acetonitrile was added for protein precipitation, and vortex-mixed (Remi, Cyclomixer, India). The denatured protein residues were removed by centrifugation (LabQuest, HMCF12VT, Borosil, India) at 5000 rpm for 10 minutes. Following centrifugation, 20 µL aliquots of the acetonitrile extract were injected directly into the HPLC system. Plasma concentrations of rilpivirine were quantified using an HPLC method employing acetonitrile and 0.1% OPA (80:20) as the mobile phase at a flow rate of 1 mL/min, with separation achieved on a C8 column [20].

Accelerated stability studies

The stability of the Rilpivirine-SLN dispersion was assessed over a 90-day period. Samples stored in glass vials were maintained under accelerated conditions (40 ± 3 °C and 75 ± 5% RH). Particle size, PDI, zeta potential, and percent drug release of the RPV-SLN formulation were evaluated at 0, 30, 60, and 90 days.

RESULT AND DISCUSSION

Selection of lipid

The selection of the lipid was primarily based on the solubility of the drug within the lipid matrix. This is because a higher solvent capacity results in a greater potential for drug loading [21] of the lipids that were used. The solubility of rilpivirine in glyceryl monostearate was found to be greater than that of other lipids, but still could not dissolve the drug completely in a ratio of 1:10 this prompted the use of glyceryl caprylate as a co-solubilizer [22]. A glyceryl caprylate, a medium-chain monoglyceride, its solubilizing effect are not merely a consequence of its amphiphilic nature, but rather a result of specific molecular interactions [23]. Its hydrophilic glycerol head and hydrophobic caprylate tail enable it to function as a surfactant, effectively lowering the interfacial tension between immiscible liquids [24].

Selection of surfactant

Table 1 summarizes the particle size and PDI results obtained from various combinations of lipid-based and aqueous surfactants. The Tween 80 and Span 80 combination was identified as optimal, producing the smallest particle size, lowest PDI, and stable SLNs. Given that both Span 80 and Tween 80 possess GRAS status, they were selected for further investigation.

Preparation of SLNs

Both the aqueous phase and lipidic phase were mixed to form pre-emulsion and processed using the hot homogenization method [13)]. The resulting formulation was allowed to cool to room temperature, yielding a drug-loaded SLN dispersion.

Determination of particle size

Corrected Proof

Table 2 presents the particle size data for the SLNs, showing a particle size distribution ranging from 47.9 to 348.6 nm. The mean particle size of optimized SLN was found to be 74.45 ± 0.84 nm with PDI 0.27. PDI value 0.3 or less indicates the uniformity in particle size. Particle size between 10-100 nm is readily absorbed in the systemic circulation through lymphatic uptake from GIT, particles size more than 100 nm are also absorbed through the lymphatic system, although more slowly [22].

Determination of zeta potential

The optimized SLN dispersion exhibited a zeta potential of −17.49 ± 0.82 mV. The charge on the nanoparticles is due to the lipid matrix i.e., glyceryl monostearate.

Zeta potential is an important factor for SLNs formulation, which affects the stability of nanoparticles. Approximately 20 mV provide only a short-term stability. However, this criterion is valid only for low–molecular–weight surfactants and systems stabilized predominantly by electrostatic mechanisms. However, Tween 80, with a molecular weight of approximately 1310 Da, is a high–molecular weight surfactant that primarily imparts steric stabilization rather than electrostatic stabilization. In this case zeta potential value of approximately 20 mV can provide sufficient stabilization [25]. It plays a key role in facilitating the lymphatic uptake of solid lipid nanoparticles. Particles exhibiting a strongly negative zeta potential (below- 30 mV) have been shown to be preferentially retained within lymph nodes by promoting M-cell uptake and accumulation in Peyer's patches, as their negative surface charge interacts with the hydrophobic membrane of M cells. [21].

Entrapment efficiency

Solid lipid nanoparticles entrapment efficiency was estimated to be between 53.9 and 71.4%. The optimized SLNs showed an entrapment efficiency of about 62.9 ± 1.2%. Glyceryl caprylate, employed as a co-solubilizer, enhanced the drug's solubility within the lipid matrix, thereby increasing entrapment efficiency.

Optimization of Rilpivirine SLNs

The Box–Behnken design was selected for optimization as it efficiently evaluates the effects of multiple independent variables while requiring fewer experimental runs. Key formulation factors lipid concentration, surfactant concentration, and the number of homogenization cycles were found to influence particle size, PDI, and entrapment efficiency. The desirability function (0.836) was probed to acquire an optimized formulation by using Design Expert software (version 13).

The software-predicted optimal SLN formulation parameters were a lipid ratio of 1:20 (6.6 g), a surfactant concentration of 2.5%, and 4.7 homogenization cycles. The ANOVA results for the Box–Behnken design used to optimize the Rilpivirine SLN formulation are presented in Table 5.

Table 5. ANOVA output of the Box-Behnken design for optimization of Rilpivirine SLNs

Sr No	Outcomes	R1 Particle Size (nm)	R2 Entrapment Efficiency (%)
1	F value	9.79	21.41
2	P value	0.0069	0.0008
3	R^2 value	0.90	0.9559
4	Adequate Precision	9.93	13.06

It was observed that no statistically significant differences existed between the predicted and experimental values for EE ($P > 0.0008$ and $P > 0.0805$), confirming the validity of the proposed model. The optimized formulation exhibited a particle size of 92 nm, a PDI of 0.27, and an entrapment efficiency of 62.9%.

Effects on particle size

By lowering the lipid concentration and increasing the surfactant concentration, a mean particle size below 100 nm was attained. An increase in the number of homogenization cycles was found to reduce particle size. Particle size is a key determinant of lymphatic uptake of nanoparticles, with the optimal range for lymphatic transport reported to be 10–100 nm. Such lymphatic absorption can enhance the oral bioavailability of lipophilic drugs by bypassing first-pass metabolism [26].

The effect on the particle size of independent variables can be explained by following Equation (3):

$$\text{Particle size} = 124.72+35.58*A-67.021*B-48.53*C-26.66*AB+15.78*AC+55.05*BC \quad (3)$$

A regression coefficient (r^2 =0.90) indicated a correlation between selected independent variables and the observed response.

The model indicates that higher lipid concentrations lead to an increase in particle size, likely due to the corresponding rise in system viscosity (Figure 1). In contrast, increasing the surfactant concentration reduces particle size by more effectively stabilizing the newly formed surfaces during homogenization (Figure 2). Additionally, the number of homogenization cycles exerts a significant influence on particle size, as increased cycles expose the formulation to greater

Corrected Proof

shear forces. All the 2-factor interactions were significant and affected the responses (Figure 3).

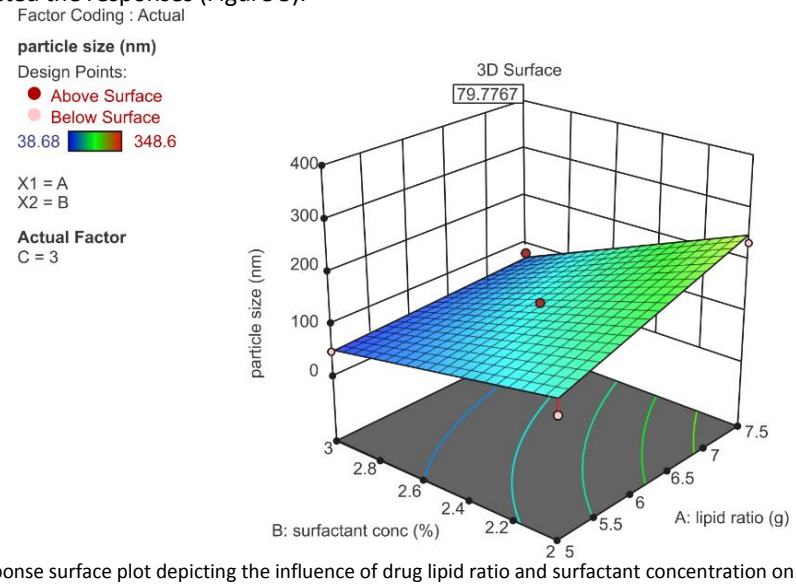

Fig. 1. Response surface plot depicting the influence of drug lipid ratio and surfactant concentration on particle size

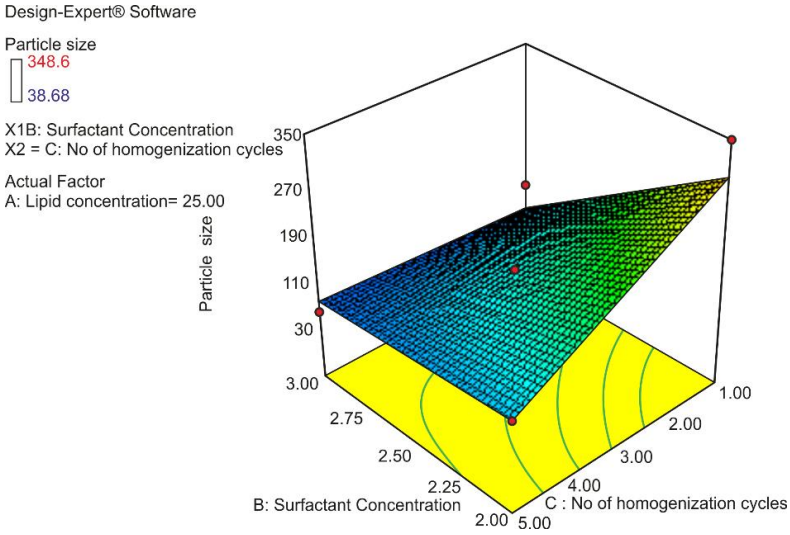

Fig. 2. Response surface plot depicting the influence of surfactant concentration and homogenization cycle on particle size

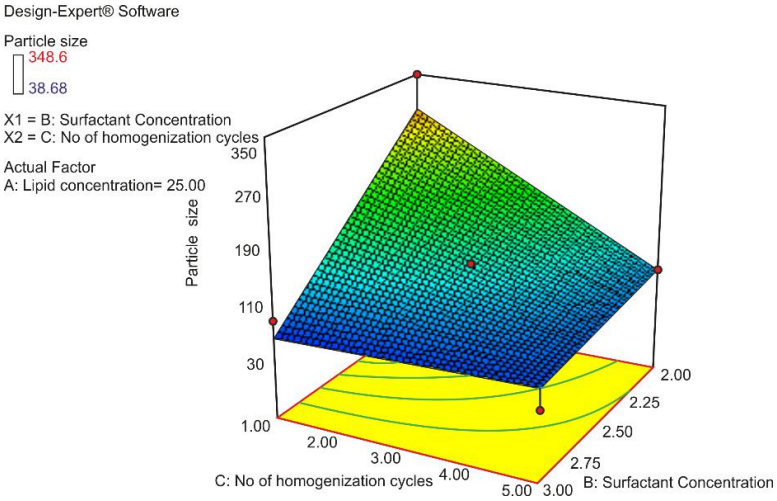

Fig. 3. Response surface plot depicting the influence of drug lipid ratio and homogenization cycle on particle size

Effects on entrapment Efficiency

Independent variables affecting entrapment efficiency can be explained by following Equation (4)

Entrapment Efficiency (EE) = +61.82+6.11A+0.9398B-0.3133C+1.25AB-1.41AC-1.88BC (4)

Increased in the amount of lipid, EE is increasing. A higher lipid content enhances drug entrapment by providing a larger matrix for incorporation (Figure 4). Increasing the surfactant concentration can also improve entrapment, likely due to additional drug incorporation within the surfactant layer (Figure 5). Conversely, increasing the number of homogenization cycles may reduce entrapment efficiency, as the resulting decrease in particle size increases the surface area available for drug diffusion into the aqueous phase (Figure 6).

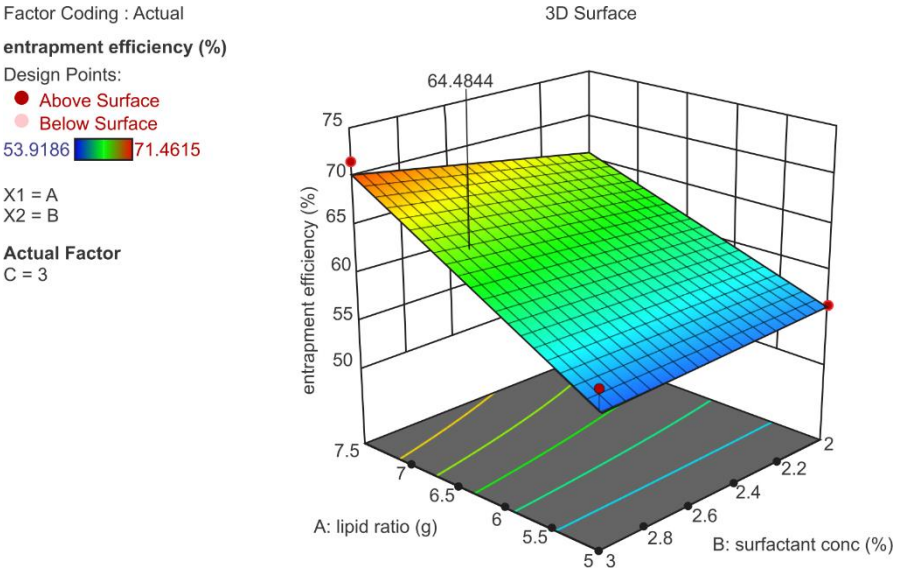

Fig. 4. Response surface plot depicting the influence of drug lipid ratio and surfactant concentration on entrapment efficiency

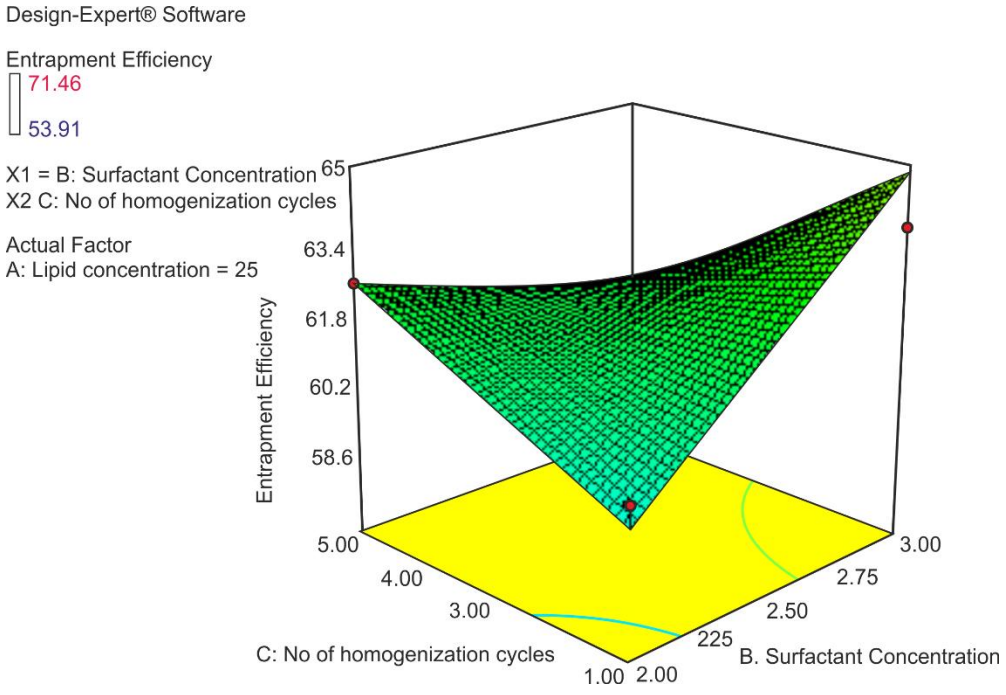

Fig. 5. Response surface plot depicting the influence of surfactant concentration and homogenization cycle on entrapment efficiency

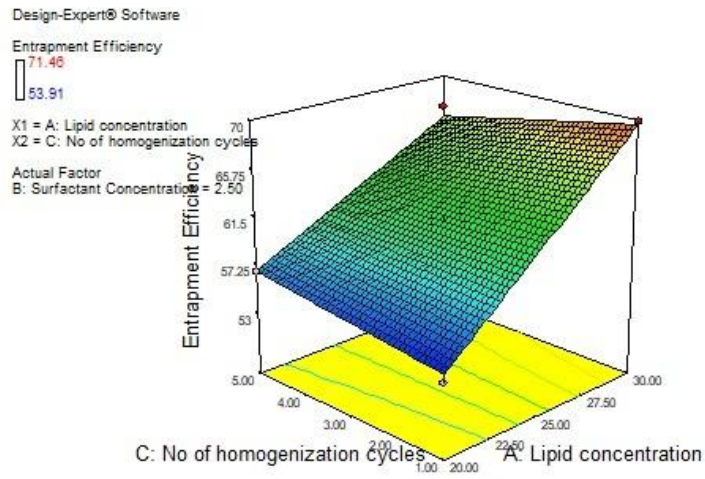

Fig. 6. Response surface plot depicting the influence of drug lipid ratio and homogenization cycle on entrapment efficiency

Surface morphology by Scanning Electron Microscopy (SEM)

Figure 7 illustrates a dense spherical configuration of optimized solid lipid nanoparticles (SLNs). Due to their symmetry in all three dimensions, spherical particles can traverse the epithelium more efficiently than ellipsoidal particles. The scanning electron microscopy (SEM) image clearly depicts SLNs with a spherical morphology.

Differential Scanning Calorimetry (DSC)

Melting points of Rilpivirine and RPV SLNs corresponds to enthalpies which are shown in Figure 8 Pure drug shows endotherm at 241 ˚C. The endothermic peak observed for RPV SLNs at approximately 70 °C indicates that rilpivirine exists in a partially crystalline, though not fully amorphous, state. The absence of the characteristic peak at 241 °C confirms the complete solubilization and uniform dispersion of rilpivirine within the molten lipid matrix. In contrast, pure crystalline rilpivirine displays a sharp melting point, reflecting the energy needed to disrupt its crystal lattice and initiate the phase transition to the liquid state [27]. When RPV was incorporated into SLNs, its physical state was altered from a crystalline to an amorphous or molecularly dispersed form within the lipid matrix. This amorphization reduces the energy required for the phase transition, leading to lower melting point [28]. Alprazolam SLN dispersion in compritol ATO 888 as a carrier had previously been observed to exhibit the behavior of conversion from crystalline to amorphous form [23].

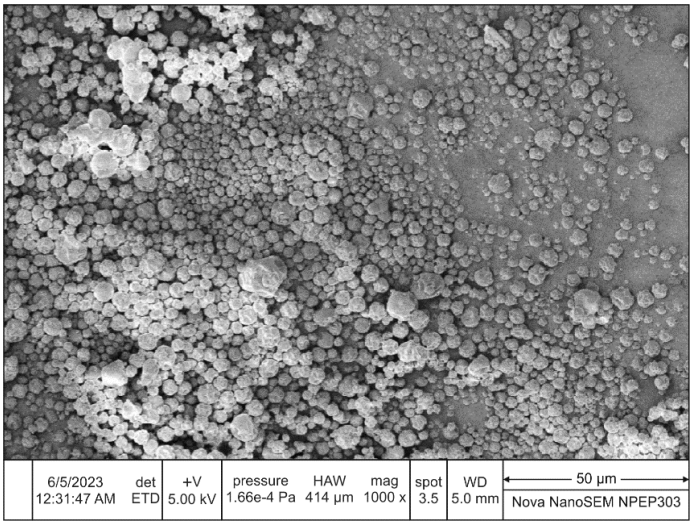

Fig. 7. SEM of Rilpivirine loaded SLNs depicts smooth spherical particles of size ranging from 64±1.78 nm to 97±2.42 nm which are suitable for lymphatic uptake

Corrected Proof

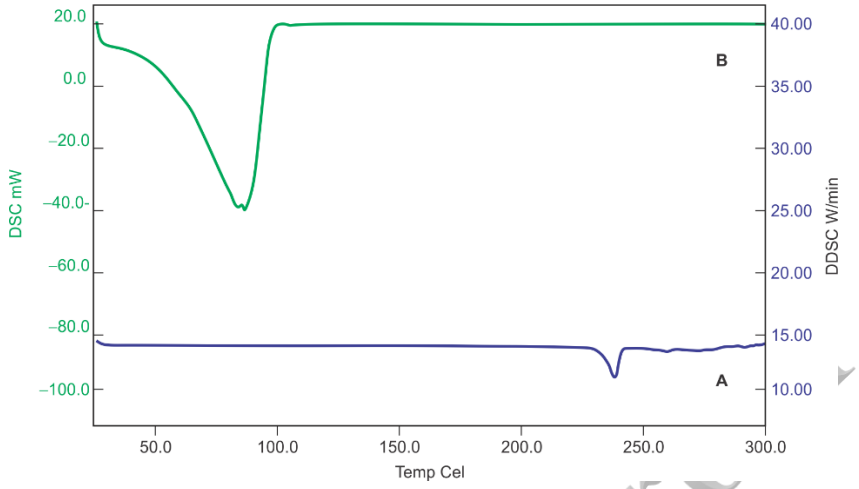

Fig. 8. Differential scanning calorimetry thermogram for A represents a thermogram of pure rilpivirine showing a sharp endothermic peak around 240-242 °C, B represents rilpivirine-loaded SLNs showing an endothermic peak around 70-80 °C which corresponds to the melting of lipid.

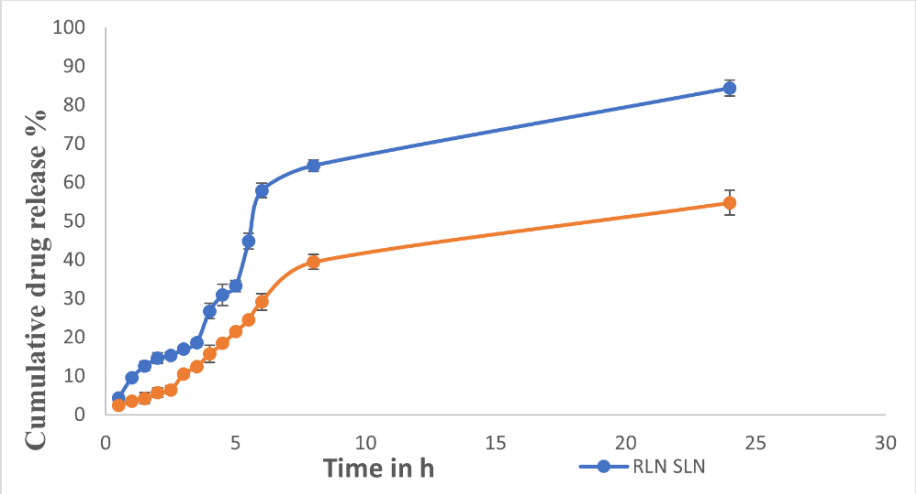

Fig. 9. *In vitro* drug release profile of RLP-SLNs and RPV suspension in phosphate buffer pH 6.8 for 24 hours. (n=3)

In vitro release of Rilpivirine

Figure 9 illustrates the in vitro release profiles of RPV SLNs and the RPV suspension. The Rilpivirine SLN dispersion was evaluated for drug release in pH 6.8 phosphate buffer containing 0.2% Tween 20 over a 24-hour period, demonstrating a sustained release pattern. The cumulative percentage release of RPV from RPV-SLNs within 24 hours was 84%, indicating a sustained release of solid lipid nanoparticles. The gradual release of nanoparticles suggests that the drug is molecularly dispersed within the lipid matrix. The kinetics of drug release in the pH 6.8 phosphate buffer followed the Korsmeyer-Peppas model, with an r^2 value of 0.975. In contrast, the RPV suspension exhibited a 54% drug release at the conclusion of 24 hours.

Ex vivo permeability study

To figure out the mechanism responsible for the uptake of SLNs, Chlorpromazine which is a lymphatic uptake blocker acts by redistributing clathrin and reducing the number of clathrin on the surface of enterocytes was used for this study. The intestinal uptake investigation of RPV SLNs were then carried out in the presence of CPZ to explore the mechanism of SLN uptake into the everted gut sac (Figure 10) depicts the apparent permeability (Papp) of RPV SLNs at 37 °C in both the presence and absence of CPZ. The results indicated that, without CPZ, the apparent permeability of RPV SLNs increased by approximately 2.8-fold compared to the permeability observed in the presence of CPZ. The addition of inhibitor considerably decreased the intestinal permeability of SLNs which indicated that the uptake of RPV SLNs may be contributed by clathrin-mediated endocytosis.

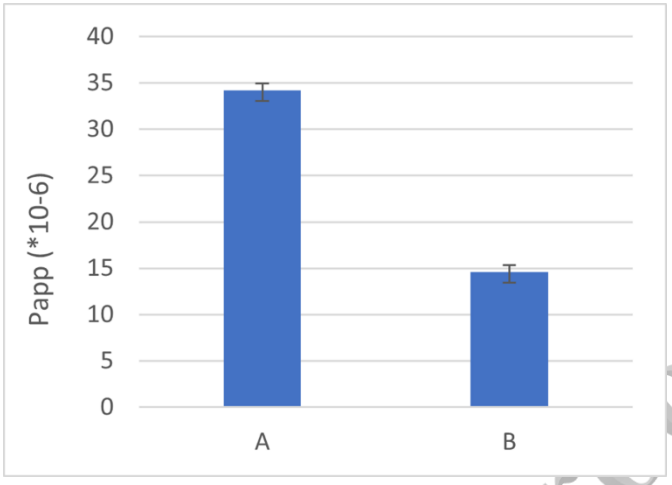

Fig. 10. *Ex-vivo* apparent permeability of rilpivirine loaded SLNs at (a) in the absence of chlorpromazine at 37 °C, (b) in the presence of chlorpromazine at 37 °C (n=3)

In Vivo pharmacokinetic study

In vivo pharmacokinetic profile for RPV SLNs was compared to RPV coarse suspension (control group) as well as the role of lymphatic uptake was studied by concurrent administration of lymphatic uptake blocker. Plasma drug concentrations were evaluated following oral administration of the RPV coarse suspension, the RPV SLN formulation (equivalent to 1 mg/kg of rilpivirine), and the RPV SLN formulation co-administered with chlorpromazine (also equivalent to 1 mg/kg of rilpivirine) (Figure 11). Represents plasma drug concentration vs time profile of SLNs coarse suspension, RPV-SLNs, and RPV SLNs with CPZ after oral administration. HPLC parameter like retention time was found to be 3.9 ± 0.8 minutes. The calibration curve was linear in the range of 0.01- 2 µg/ml (r^2=0.993). Various pharmacokinetic parameters were calculated and noted in Table 6. It is evident from Figure 11 that the plasma concentration of CPZ-treated rats was found to be lesser as compared to that of the control group (CPZ non-treated). The C_{max} of the SLNs formulation was two times higher when compared to RPV Coarse suspension and RPV SLNs with CPZ. The AUC of the SLN formulation was significantly higher than that of the RPV coarse suspension. The oral administration of RPV SLNs resulted in an $AUC_{0-\infty}$ approximately 2.47-fold greater than that of the suspension. This enhanced AUC may be attributed to reduce first-pass metabolism one of the primary factors contributing to the drug's low bioavailability along with lymphatic uptake and improved dissolution. The M cells of the intestinal epithelium prefer to take up drugs that are entrapped in lipids, which increases the permeability of the SLNs over bulk drug. The increased bioavailability and higher plasma concentration of rilpivirine were attributed to several factors, such as particle size of SLNs, and improved dissolution, SLNs was administered along with CPZ demonstrating that an important role played by the clathrin-mediated endocytosis, present in the enterocytes, and an improvement in lipid uptake by lymphatic transport due to the presence of GMS and surfactant.

These animal study will help as a supportive data for further clinical study.

Table 6. Pharmacokinetic parameters of Rilpivirine after oral administration of RPV coarse suspension and RPV-SLNs to Wistar rats (n=3)

Parameters	RPV Coarse suspension	RPV SLNs	RPV SLNs with CPZ
C_{max}	252.8± 8.15 ng/ml	455 ± 2.44 ng/ml	315.2± 5.46 ng/ml
T_{max}	4 hrs.	4 hrs.	4hrs.
$K_{.e}$ (h^{-1})	0.019	0.541	0.012
AUC_{0-t}	4266.54	5016.533	2156.95
$AUC_{t-\infty}$	1025.6	848.107	622.4
$AUC_{0-\infty}$	5291.601	5544.984	2779.35

Corrected Proof

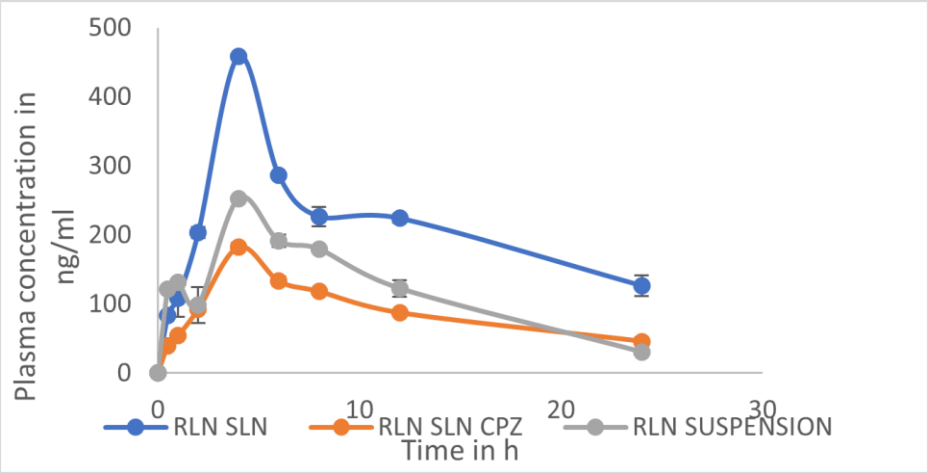

Fig. 11. Plasma concentration-time profile of Rilpivirine in wistar rats after oral administration of Rilpivirine coarse suspension, Rilpivirine SLNs, and Rilpivirine SLNs with chlorpromazine for 24 hours (n=6)

Table 7. Stability study data for RLV-SLNs

Sr No.	Parameters	0 days	30 days	60 days	90 days
1	Particle size(nm)	75.02 ± 0.84	78.03 ± 0.95	79 ± 0.47	81.7 ± 1.24
2	Zeta potential(mV)	-17.49 ± 1.82	- 18.46 ± 1.6	-18.89 ± 1.57	-19.91 ± 2.01
3	PDI	0.27 ± 0.04	0.29 ± 0.06	0.35 ± 0.05	0.36 ± 0.04
4	Drug release	84 ± 2.4%	82 ± 1.9%	81.1 ± 2.1 %	79.1 ± 1.2%

Accelerated stability

According to ICH criteria, the stability of the formulation was evaluated under storage condition of 40 °C ± 75 % RH. SLNs stability was estimated using particle size, PDI, and zeta potential. Results showed that none of the evaluated factors had changed significantly. Table 7 displays the results of the accelerated stability investigation. Insignificant increase in the particle size of SLNs at the end of 90 days. During storage, the entrapment efficiency of SLN showed insignificant reduction which indicated that the drug was retained in the lipid nanoparticles for 90 days of storage. PDI of SLN dispersion remained almost constant during storage. There was no significant change in % drug release during storage.

CONCLUSION

The results of this investigation confirm that solid lipid nanoparticles (SLNs) constitute an effective approach for improving oral bioavailability. In this investigation, Rilpivirine SLNs were synthesized utilizing the high-pressure homogenization (HPH) method. Multiple formulations were prepared and assessed using the Box–Behnken design to optimize both particle size and entrapment efficiency. The use of glyceryl monostearate, in conjunction with a co-solubilizer and the surfactants SPAN 80 and Tween 80, resulted in nanoparticles with enhanced stability. Ex-vivo intestinal permeability studies elucidated the role of lymphatic uptake via the clathrin-mediated endocytosis mechanism of SLNs in augmenting bioavailability. The in vivo pharmacokinetic evaluation revealed that oral administration of the SLNs resulted in higher Cmax and AUC values compared with the control suspension. The role of lymphatic uptake was further investigated through the concurrent administration of a lymphatic uptake blocker alongside the SLNs formulation. In conclusion, bypassing first-pass metabolism together with enhanced lymphatic uptake achieved through SLNs can substantially improve the oral bioavailability of rilpivirine, potentially enabling dose reduction and improved patient compliance.

Future work and limitations

The extension of present work can be performing cytotoxicity assay (CCK-8/MTS) using intestinal epithelial cells and long term stability studies which can be undertaking in future.

ACKNOWLEDGMENT

The authors sincerely thank the Principal of AISSMS College of Pharmacy, Pune, for offering the required support and facilities for conducting this research work.

FUNDING

The authors declare that this project received no external funding.

Corrected Proof

CONFLICT OF INTEREST

The authors declare that they have no conflicts of interest related to this study.

REFERENCES

1. Govender RD, Hashim MJ, Khan MA, Mustafa H, Khan G. Global epidemiology of HIV/AIDS: A resurgence in North America and Europe. J Epidemiol Glob Health. 2021;11(3):296–301.
2. Hammer SM, Saag MS, Schechter M, Montaner JSG, Schooley RT, Jacobsen DM, et al. Treatment for adult HIV infection: 2006 recommendations of the International AIDS Society-USA panel. JAMA. 2006;296 (7):827–843.
3. James C, Preininger L, Sweet M. Rilpivirine: a second-generation nonnucleoside reverse transcriptase inhibitor. Am J Health-Syst Pharm AJHP Off J Am Soc Health-Syst Pharm. 2012;69 (10):857–861.
4. Seneviratne HK, Tillotson J, Lade JM, Bekker LG, Li S, Pathak S, et al. Metabolism of long-acting rilpivirine after intramuscular injection: HIV prevention trials network study 076 (HPTN 076). AIDS Res Hum Retroviruses. 2021;37(3):173–183.
5. Zainuddin R, Zaheer Z, Sangshetti JN, Momin M. Enhancement of oral bioavailability of anti-HIV drug rilpivirine HCl through nanosponge formulation. Drug Dev Ind Pharm. 2017; 43 (12):2076–2084.
6. kommavarapu P, Maruthapillai A, Palanisamy K, Sunkara M. Preparation and characterization of rilpivirine solid dispersions with the application of enhanced solubility and dissolution rate. Beni-Suef Univ J Basic Appl Sci. 2015;4(1):71–79.
7. Suresh G, Manjunath K, Venkateswarlu V, Satyanarayana V. Preparation, characterization, and in vitro and in vivo evaluation of lovastatin solid lipid nanoparticles. AAPS PharmSciTech. 2007; 8(1):E162–E170 .
8. Makwana V, Jain R, Patel K, Nivsarkar M, Joshi A. Solid lipid nanoparticles (SLN) of efavirenz as lymph targeting drug delivery system: elucidation of mechanism of uptake using chylomicron flow blocking approach. Int J Pharm. 2015;495(1):439–446.
9. Bhalekar MR, Upadhaya PG, Madgulkar AR, Kshirsagar SJ, Dube A, Bartakke US. In-vivo bioavailability and lymphatic uptake evaluation of lipid nanoparticulates of darunavir. Drug Deliv. 2016;23(7):2581–2586.
10. Trevaskis NL, Charman WN, Porter CJH. Lipid-based delivery systems and intestinal lymphatic drug transport: a mechanistic update. Adv Drug Deliv Rev. 2008;60(6):702–716.
11. Silva AC, González-Mira E, García ML, Egea MA, Fonseca J, Silva R, et al. Preparation, characterization and biocompatibility studies on risperidone-loaded solid lipid nanoparticles (SLN): high pressure homogenization versus ultrasound. Colloids Surf B Biointerfaces. 2011;86(1):158–165.
12. Hao J, Fang ,Xinsheng, Zhou ,Yanfang, Wang ,Jianzhu, Guo ,Fengguang, Li ,Fei, et al. Development and optimization of solid lipid nanoparticle formulation for ophthalmic delivery of chloramphenicol using a Box-Behnken design. Int J Nanomedicine. 2011;6: 683–692.
13. Varshosaz J, Tabbakhian M, Mohammadi MY. Formulation and optimization of solid lipid nanoparticles of buspirone HCl for enhancement of its oral bioavailability. J Liposome Res. 2010; 20(4):286–296.
14. Chadha R, Bhandari S. Drug-excipient compatibility screening--role of thermoanalytical and spectroscopic techniques. J Pharm Biomed Anal. 2014;87:82–97.
15. Ebrahimi HA, Javadzadeh Y, Hamidi M, Jalali MB. Repaglinide-loaded solid lipid nanoparticles: effect of using different surfactants/stabilizers on physicochemical properties of nanoparticles. Daru. 2015;23 (1):46-56.
16. Ravi PR, Vats R, Dalal V, Murthy AN. A hybrid design to optimize preparation of lopinavir loaded solid lipid nanoparticles and comparative pharmacokinetic evaluation with marketed lopinavir/ritonavir coformulation. J Pharm Pharmacol. 2014;66(7):912–926.
17. Lind ML, Jacobsen J, Holm R, Müllertz A. Intestinal lymphatic transport of halofantrine in rats assessed using a chylomicron flow blocking approach: the influence of polysorbate 60 and 80. Eur J Pharm Sci Off J Eur Fed Pharm Sci. 2008;35(3):211–218.
18. Pouton CW. Formulation of poorly water-soluble drugs for oral administration: physicochemical and physiological issues and the lipid formulation classification system. Eur J Pharm Sci. 2006;29(3–4):278–287.
19. Bhalekar M, Upadhaya P, Madgulkar A. Formulation and characterization of solid lipid nanoparticles for an anti-retroviral drug darunavir. Appl Nanosci. 2017;7(1):47–57.
20. Kumar BMS, Rajkamal B, Chandramowli B. Development and validation of rilpivirine in pharmaceutical formulation by RP-HPLC. Am J PharmTech Res. 2019;9(3):344–353.
21. Ali Khan A, Mudassir J, Mohtar N, Darwis Y. Advanced drug delivery to the lymphatic system: lipid-based nanoformulations. Int J Nanomedicine. 2013;8:2733–2744.
22. Mahmoudian M, Valizadeh H, Zakeri-Milani P. Bortezomib-loaded solid lipid nanoparticles: preparation, characterization, and intestinal permeability investigation. Drug Dev Ind Pharm. 2018;44(10):1598–1605.
23. Tadros T. Chapter 2 - Colloid and interface aspects of pharmaceutical science. In Colloid and interface science in pharmaceutical research and development. 2014:29-54
24. Shafiq S, Shakeel F, Talegaonkar S, Ahmad FJ, Khar RK, Ali M. Development and bioavailability assessment of ramipril nanoemulsion formulation. Eur J Pharm Biopharm. 2007;66(2):227–243.
25. Honary S, Zahir F. Effect of zeta Potential on the properties of nano-drug delivery systems - A review (Part 2). Trop J Pharm Res. 2013;12(2):265–273.
26. Huma R, Saeed A, Asadullah M, Iqra R, Mohammed G, Umme H, et al. Compritol-based alprazolam solid

Corrected Proof

lipid nanoparticles for sustained release of alprazolam: preparation by hot melt encapsulation. Molecules. 2022;27(24):8894.
27. Karla L, Andrea R, Jose A, Flavia Z. Solid lipid nanoparticles (SLN) and nanostructured lipid carriers (NLC) prepared by microwave and ultrasound-assisted synthesis: promising green strategies for the nanoworld. Pharmaceutics. 2023;15(5):1333.
28. Carine P, Fabiola M, Jelver R, Frederico P, Adny S, Paula S, Angela C, Tania P. Influence of surfactant and lipid type on the physicochemical properties and biocompatibility of solid lipid nanoparticles. Int J Environ Res Public Health. 2014; 11(8): 8581-8596.

Corrected Proof